

Development and validation of an immune-related gene pairs signature in lower-grade glioma

Xu Zhang

Department of Neurosurgery, General Hospital of Ningxia Medical University, Yinchuan

Shuai Ping

Department of Orthopedics, Liyuan Hospital, Tongji Medical College, Huazhong University of Science and Technology, Wuhan

Rui Zhang

Ningxia Key Laboratory of Cerebrocranial Disease, Incubation Base of National Key Laboratory, Ningxia Medical University, Yinchuan

Can Li

Department of Neurosurgery, General Hospital of Ningxia Medical University, Yinchuan

Caibin Gao

Department of Neurosurgery, General Hospital of Ningxia Medical University, Yinchuan

Hui Ma

Department of Neurosurgery, General Hospital of Ningxia Medical University, Yinchuan

Tao Sun

Department of Neurosurgery, General Hospital of Ningxia Medical University, Yinchuan

Feng Wang (✉ nxwwang@163.com)

Department of Neurosurgery, General Hospital of Ningxia Medical University, Yinchuan

<https://orcid.org/0000-0003-2268-0943>

Research

Keywords: glioma, prognosis, immune-related gene pairs

Posted Date: June 18th, 2020

DOI: <https://doi.org/10.21203/rs.3.rs-35147/v1>

License:   This work is licensed under a Creative Commons Attribution 4.0 International License.

[Read Full License](#)

Abstract

Background

Lower-grade gliomas (LGG) are the prevalent primary intracerebral malignancy tumor. Increasing evidence indicated an association between immune signature and LGG prognosis. Thus, we aim to develop an immune-related gene pairs (IRGPs) signature that can predict prognosis for LGG.

Method:

Gene expression levels and clinical information of LGG patients (LGGs) were collected from The Cancer Genome Atlas (TCGA) and Chinese Glioma Genome Atlas (CGGA) databases. The two databases were divided into training cohort ($n = 515$) and an independent validation cohort ($n = 604$). IRGPs significantly associated with prognosis were selected by Cox regression. Gene set enrichment analysis and filtration were performed on IRGPs.

Results

Within 1991 immune genes, an 8 IRGPs signature including 15 unique genes was constructed, which had a significant association with survival. In the validation dataset, the IRGPs signature significantly stratified LGGs into low- and high-risk groups ($P < 0.001$), and it remained an independent prognostic factor in univariate and multivariate analyses ($P < 0.001$). Additionally, 26 functional pathways were filtrated through the intersection of Gene set enrichment analysis (GSEA) and gene ontology (GO) enrichment analysis.

Conclusion

The IRGPs signature demonstrated good prognostic value in lower-grade glioma, which may provide new insights into individual treatment for glioma patients. And the IRGPs might take effect through these filtrated 26 functional pathways.

Background

Lower-grade gliomas (LGG), consisting of the World Health Organization (WHO) grades II and III, are the prevalent primary intracerebral malignancy tumor[1]. To date, surgical resection combined with postoperative chemoradiotherapy is the standard treatment for LGG. Although a lot of effort has been put forth to improve the clinical outcome, more than half of the LGGs experience recurrence or progress to high-grade glioma over time[2]. What's more, in addition to conventional surgical therapy, LGGs has limited sensitivity to chemotherapy and radiation[3, 4]. Thus, there may exist other prognostic factors for LGG. Several biomarkers, including co-deletion of chromosome arms 1p and 19q (1p/19q co-deletion), O-

6-methylguanine-DNA methyltransferase (MGMT) methylation and isocitrate dehydrogenase (IDH) mutation have been added to the 2016 WHO classification, to clarify the histological features and to guide the therapeutic plan[5–8]. However, these widely recognized biomarkers cannot properly evaluate individual risk stratification in LGG.

Tumor microenvironment (TME) has drawn a lot of attention as a vital cellular milieu for its pivotal roles in tumor initiation, progression, and metastasis. It consists of mesenchymal cells, inflammatory mediators endothelial cells, as well as immune cells and stromal cells[9]. Additionally, immune cells and stromal cells are two main non-tumor components, which have great importance in the diagnosis and prognosis of tumors[10]. A prevalent algorithm called ESTIMATE designed by Yoshihara et al. has been used to evaluate immune cells and stromal cells in many malignant tumors[11–13]. In this study, we also employed this algorithm for further research.

Glioma immune microenvironment matters in glioma biology[14]. Immune-checkpoint inhibitors and immunotherapy play a part in improving gliomas prognosis[15, 16]. As to prognosis biomarkers, researchers have explored the possibility of stratifying patients with malignant tumors (including gliomas) based on gene expression profiles and have constructed a multigene-expression model that can be applied to stratify high-risk subgroup[17–22]. One common drawback of the above studies is that gene expression profiles require suitable normalization. There exists an inevitable deviation owing to technical biases across sequencing platforms and biological heterogeneity[23]. Thus, researchers have invented the conception of immune-related gene pairs, which can eliminate the disadvantages of data processing and is considered to be a robust prognostic indicator in some tumors[24–29].

However, its prognostic value has not been estimated in lower-grade glioma. In our study, we constructed and validated a personal prognostic indicator by integrating immune-related gene pairs for lower-grade glioma.

Materials And Methods

Acquisition of LGG expression profiles from TCGA and CGGA datasets

The RNA-seq Fragments Per Kilobase per Million(FPKM) expression and clinical data of 515 LGG patient samples were downloaded and selected from the TCGA database (<https://portal.gdc.cancer.gov>); The mRNA Sequencing and clinical data of 604 LGG samples were downloaded from the CGGA dataset (<http://www.cgga.org.cn>).

Acquisition of immune-related genes

We downloaded a comprehensive list of immune-related genes (IRGs) from the Immunology Database and Analysis Portal (ImmPort) database (<https://www.immport.org>). Then, the limma package of R software was utilized to extract the RNA expression profiles of IRGs (determined by median absolute

deviation, $MAD > 0.5$)[30]. We select co-expressed IRGs both in TCGA and CGGA databases for further study.

Establishment of prognostic signature based on the immune-related genes pairs

A pairwise comparison was played between the immune-related gene expression levels in each sample to acquire a score for each IRGP. An IRGP was counted as follows: (1) if $IRG_1 > IRG_2$, $IRGP = 1$; (2) if $IRG_1 < IRG_2$, $IRGP = 0$. The superiority of analyzing genes in a pairwise method is that it eliminates the need for normalization steps for individualized analysis[29]. If the score of an IRGP was 0 or 1 in more than 80% of the samples of the TCGA dataset or the CGGA dataset, then we discarded the IRGP. Then we apply Least absolute shrinkage and selection operator (LASSO) Cox regression (iteration = 1000) to generate an IRGP index (IRGPI) by using R package glmnet. In order to stratify patients into high and low-risk groups, the optimal cut-off value of the IRGPI was determined using receiver operating characteristic (ROC) curve analysis at 3-year overall survival in the TCGA database.

Validation of the IRGPI

We further evaluated the IRGPI model in the CGGA database of LGG samples by the log-rank test. Additionally, we assessed the IRGPI together with other clinical variables in the univariate and multivariate cox proportional hazard regression model in TCGA and CGGA datasets.

Profiling of infiltrating immune cells

To clarify immune cell infiltration in a different risk group, we used CIBERSORT[31], a popular algorithm for exploring cell composition of tumor tissues from their gene expression profiles. Gene expression profile was uploaded to the online analytical platform CIBERSORT web portal (<http://cibersort.stanford.edu>), using the default signature matrix at 1,000 permutations. Then, The p-values were calculated by using 'wilcox.test' function in R.

Gene set enrichment analysis and the filtration of the results

To understand the biological functions of this immune-related prognostic signature, we employed gene set enrichment analysis (GSEA/MSigDB, <http://software.broadinstitute.org/gsea/downloads.jsp>). FalseDiscovery Rate-adjusted $P < 0.05$ was considered statistically significant. To make a comprehensive understanding of some biological functions, we filter the outcome of GSEA from the perspective of the tumor microenvironment. Scores of immune and stromal were calculated using the ESTIMATE algorithm^[11], immune scores and stromal scores were stratified into low-level groups and high-level groups according to the median value, respectively. Then we acquired the intersected differentially expressed genes (DEGs) among stromal scores and immune scores, which exhibited by the VennDiagram package[32]. Additionally, we conducted gene ontology (GO) enrichment analysis based on the DEGs. Finally, we took an intersection between GO and GSEA by using the Venn Diagram package.

Statistical analysis

All statistical analyses were performed using R software (version 3.5.1, <https://www.r-project.org>). For all tests, a p -value < 0.05 indicated a statistically significant difference. Statistical significance is shown as $*P < 0.05$, $**P < 0.01$, $***P < 0.001$.

Result

Prognostic IRGPs signature construction

To make our investigation process more explicit, the entire workflow is illustrated in Fig. 1. A total of 1,119 patients with LGG were included in the analysis (Additional file 1: Table S1). TCGA cohort was used as the training dataset. Altogether, 1991 immune-related genes (IRGs) were downloaded from the ImmPort database (accessed on 10/5/2020). 372 IRGs were measured both in TCGA and CGGA datasets (MAD > 0.5).

From these 372 IRGs, 15,245 IRGPs were constructed. After discarding IRGPs with relatively small variation (MAD = 0), 22 IRGPs were left and chosen as initial candidate IRGPs. Then we defined IRGPI by Lasso Cox proportional hazards regression on the training set and selected 8 IRGPs in the final model. The IRGPI consisted of 15 unique IRGs (Table 1). The optimal cut-off value of the IRGPI for prediction of LGG prognosis was determined to be -0.007 using the ROC curve analysis (Fig. 2). The IRGPI significantly stratified patients into low- and high-risk groups in terms of overall survival (OS). We found the high-risk group had a significantly more inferior OS than the low-risk group in the TCGA cohort ($P < 0.001$, Fig. 3a). To further investigate the prognostic value of the IRGPI, we applied uni- and multivariate Cox regression analyses to the training cohort. After combining with the clinical factors such as age, sex, and tumor grade. The risk score of IRGPI remained an independent prognostic factor ($P < 0.001$, HR, 2.467 [2.003, 3.037]; Fig. 3c, e).

Table 1
Model information about IRGPI

IRG1	Immune processes	IRG2	Immune processes	Coefficient
PLSCR1	Antimicrobials	BMP2	Cytokines	0.41
BIRC5	Antimicrobials	KLRC2	Antigen Processing and Presentation	0.06
OAS1	Antimicrobials	CXCL12	Antimicrobials	0.78
PPP3CB	BCR Signaling Pathway	FAM3C	Cytokines	-0.67
EDNRA	Cytokine Receptors	OSMR	Cytokine Receptors	-0.29
PLAUR	Cytokine Receptors	PGF	Cytokines	0.67
BMP2	Cytokines	NRP2	Cytokine Receptors	-0.02
NRG3	Cytokines	NR2E1	Cytokine Receptors	-0.49

Validation of the IRGPI for survival prediction

To confirm whether the IRGPI had consistent prognostic value in different populations, we applied the IRGPI signature to the CGGA database (n = 604) as external validation. Unsurprisingly, On the CGGA cohort, the high-risk group had a significantly shorter OS than the low-risk patients ($P < 0.001$, Fig. 3b).

Additionally, it also remained an independent prognostic factor when taking clinical factors such as age, sex, and tumor grade into consideration ($P < 0.001$, HR, 1.873 [1.653, 2.122]; Fig. 3d, f).

Immune cells infiltration between different risk groups

To gain a better insight into the difference of immune cells infiltration between the low-risk and high-risk groups, we carried out immune infiltration analysis. Figure 4a presented a comparative summary of the CIBERSORT outcome resulting from the two risk groups. We found Macrophage M1 and T cells CD8 were significantly highly expressed in the high-risk group ($P = 1.757e-04$, Fig. 4b; $P = 0.002$, Fig. 4d), while Monocytes was significantly highly expressed in the low-risk group ($P = 5.749e-05$, Fig. 4c). What's more, Macrophage M0 and T cells CD4 memory activated were also highly expressed in the high-risk group in our study ($P = 0.004$, Additional file 3: Fig S1a; $P = 0.033$, Additional file 3: Fig S1b).

Gene set enrichment analysis and the filtration of the results

We carry out GSEA between low- and high-risk groups to explore the pathways that were significantly altered. And we found 299 pathways were significantly different (Additional file 2: Table S2). Then we selected the 50 minimum adjusted P -pathways for filtration. According to statistics, 1199 up-regulated DEGs and 296 down-regulated DEGs were selected in the stromal score group. While 965 up-regulated DEGs and 692 down-regulated DEGs were selected in the immune score group. Then, 887 up-regulated intersected genes and 277 down-regulated intersected genes were revealed in Venn plots (Fig. 5a,b). The gene ontology (GO) analysis of these intersected genes was exhibited in Fig. 5c. Finally, we took an intersection between GO and GSEA. As a result, 26 functional pathways were filtrated (Fig. 6, Table 2).

Table 2
The intersection functional pathways between GO and
GSEA

Functional pathways
1. leukocyte migration
2. regulation of lymphocyte activation
3. positive regulation of cell activation
4. positive regulation of cytokine production
5. regulation of immune effector process
6. positive regulation of cell adhesion
7. lymphocyte differentiation
8. cell chemotaxis
9. negative regulation of immune system process
10. response to molecule of bacterial origin
11. regulation of inflammatory response
12. response to virus
13. regulation of hemopoiesis
14. extracellular structure organization
15. myeloid cell differentiation
16. coagulation
17. regulation of peptidase activity
18. regulation of vasculature development
19. viral life cycle
20. negative regulation of proteolysis
21. negative regulation of hydrolase activity
22. ossification
23. positive regulation of response to biotic stimulus
24. vesicle lumen
25. endoplasmic reticulum lumen
26. enzyme inhibitor activity

Discussion

In the present study, we constructed an immune-related gene pairs signature and validated this signature in the external dataset. Our research showed the signature could stratify patients into low- and high-risk groups. Uni- and multivariate Cox regression analyses showed that the risk score was an independent prognostic factor. The prognostic signature related to tumor immune microenvironment may disclose a new perspective to develop a novel predictive biomarker and improve LGG patient management in the era of immunotherapy.

Similar to other studies, several immune cells distributed significantly differently in our research. For example, we found T cells CD8 and Macrophage M0 are significantly enriched in the high-risk group, Wu et al.'s research[27] also have the same trend, though was not statistically significant. While the opposite view indicated T cells CD8 was significantly higher in the low-risk group[28]. This phenomenon may be because the selected immune-related gene pairs and tumor types are different from each other in the above researches. Thus it needs further exploration. Additionally, we filtrated 26 functional pathways from the intersection between GO and GSEA, and this may indicate these immune-related gene pairs take effect through these functions.

Despite a better prognosis for LGG patients (LGGs), 70% of them inevitably progress to high-grade aggressive gliomas and eventually result in death[33]. Over the past 30 years, the overall survival of the majority LGGs had not been significantly improved[2]. Thus, it is vital to develop an individualized treatment protocol for LGG. Reliable prognostic biomarkers could identify patients with poor outcomes and who might benefit from intensive therapy. Recently, significant research on immune-related genes (IRGs) expression has shown great prognostic value in LGG. For example, Deng et al.[34] found up to 397 IRGs were significantly associated with LGG survival. Zhang et al.[21] established a risk model based on 6 IRGs (CANX, HSPA1B, KLRC2, PSMC6, RFXAP, and TAP1). However, one common disadvantage of all the above assays lies in standardizing gene expression profiles, which is difficult to avoid. The immune-related gene pairs signature depends on relative ranking and paired comparison of gene expression profile within a sample. This strategy is in favor of dealing with combined gene expression profiles from multiple databases. LGGs can be further divided into subgroups with different survival outcomes by this prognostic immune signature. So our signature can evaluate LGGs prognosis in a single-sample, individualized form.

Our 8-IRGP signature consists of 15 immune-related genes, and these genes play a vital role in the regulation of the immune microenvironment. Bone morphogenetic protein 2 (MP2) is known to facilitate differentiation and growth inhibition in glioma through the downregulation of both O6-methylguanine-DNA methyltransferase (MGMT) and hypoxia-inducible factor-1a (HIF-1a)[35]. It was reported that killer cell lectin-like receptor subfamily C, member 2 (KLRC2), a transmembrane activating receptor of natural killer cells, expressed higher in glioma-initiating cells compared with neural stem cell lines and normal adult brain tissue[36]. Emerging evidence suggests that the chemokine (C-X-C motif) ligand 12 (CXCL12), which is secreted from glioma stem cells (GSCs), plays a vital role in tumorigenesis and proliferation[37].

Additionally, many of the selected 26 functional pathways are related to the immune microenvironment, such as regulation of immune effector process, positive regulation of cytokine production, and cell chemotaxis. Researches had shown that numerous cytokines and chemokines promote the infiltration of various cells: circulating progenitor cells, endothelial cells, and a range of immune cells such as peripheral macrophages, microglia, leukocytes, CD4 + T cells into the glioma[38–40]. These non-neoplastic cells have an important role in tumor growth, metastasis, as well as response to treatment[14]. Thus these functional pathways matter in glioma immune microenvironment.

There are also some limitations to this study. First, the immune-related gene expression profiles are determined by RNA-seq, which is hard to generalize in daily clinical applications for its sophisticated detection program and high price. Second, the immune signature comes from fresh frozen samples. Thus, there are still doubts about the efficiency and stability. Finally, our study was a retrospective analysis, and prospective research is needed to validate the results.

Conclusion

Taken together, we systematically estimated the prognostic value of the new IRGP prognostic model, which may provide a legitimate approach in LGG management. And this may become a valuable predictive tool to identify patients who may benefit from immunotherapy. Additionally, we filtrated 26 functional pathways from the intersection between GO and GSEA, indicating these immune-related gene pairs may take effect through these functions.

Abbreviations

LGG: Lower-grade gliomas; LGGs: Lower-grade gliomas patients; IRG: immune-related gene; IRGs: immune-related genes; IRGP: immune-related gene pair; IRGPs: immune-related gene pairs; IRGPI: immune-related gene pair index; TCGA: The Cancer Genome Atlas database; CGGA: The Chinese Glioma Genome Atlas database; GSEA: Gene set enrichment analysis; GO: gene ontology; DEGs: differentially expressed genes.

Declarations

Ethics approval and consent to participate

Ethical approval was waived by the local Ethics Committee of Ningxia Medical University for the data of patients are downloaded from public databases.

Consent for publication

Not applicable

Availability of data and materials

The datasets generated and analysed during the current study are available in the TCGA (<https://portal.gdc.cancer.gov>) and CGGA (<http://www.cgga.org.cn>) repositories.

Competing interests

The authors declare that they have no competing interests.

Funding

This work was supported by grants from the Key Research and Development Program of Ningxia Hui Autonomous Region (2018BFG02007).

Authors' contributions

Feng Wang, Tao Sun and Hui Ma contributed to the study conception and design. Data collection was performed by Xu Zhang, Can Li, Caibin Gao. Data analysis was performed by Shuai Ping. The first draft of the manuscript was written by Xu Zhang and Rui Zhang, and all authors commented on previous versions of the manuscript. All authors read and approved the final manuscript.

Acknowledgements

Not applicable

References

1. Ostrom QT, Gittleman H, Farah P, Ondracek A, Chen Y, Wolinsky Y, Stroup NE, Kruchko C, Barnholtz-Sloan JS. CBTRUS statistical report: Primary brain and central nervous system tumors diagnosed in the United States in 2006–2010. *Neuro Oncol.* 2013;15(Suppl 2):ii1–56.
2. Claus EB, Walsh KM, Wiencke JK, Molinaro AM, Wiemels JL, Schildkraut JM, Bondy ML, Berger M, Jenkins R, Wrensch M. Survival and low-grade glioma: the emergence of genetic information. *Neurosurgical Focus* 2015, 38.
3. Yan Y, Li Z, Zeng S, Wang X, Gong Z, Xu Z. FGFR2-mediated phosphorylation of PTEN at tyrosine 240 contributes to the radioresistance of glioma. *J Cell Commun Signal.* 2019;13:279–80.
4. Yan Y, Xu Z, Dai S, Qian L, Sun L, Gong Z. Targeting autophagy to sensitive glioma to temozolomide treatment. *J Exp Clin Cancer Res.* 2016;35:23.
5. Louis DN, Perry A, Burger P, Ellison DW, Reifenberger G, von Deimling A, Aldape K, Brat D, Collins VP, Eberhart C, et al. International Society Of Neuropathology–Haarlem consensus guidelines for nervous system tumor classification and grading. *Brain Pathol.* 2014;24:429–35.

6. Hartmann C, Hentschel B, Wick W, Capper D, Felsberg J, Simon M, Westphal M, Schackert G, Meyermann R, Pietsch T, et al. Patients with IDH1 wild type anaplastic astrocytomas exhibit worse prognosis than IDH1-mutated glioblastomas, and IDH1 mutation status accounts for the unfavorable prognostic effect of higher age: implications for classification of gliomas. *Acta Neuropathol.* 2010;120:707–18.
7. Louis DN, Perry A, Reifenberger G, von Deimling A, Figarella-Branger D, Cavenee WK, Ohgaki H, Wiestler OD, Kleihues P, Ellison DW. The 2016 World Health Organization Classification of Tumors of the Central Nervous System: a summary. *Acta Neuropathol.* 2016;131:803–20.
8. Wick W, Meisner C, Hentschel B, Platten M, Schilling A, Wiestler B, Sabel MC, Koeppen S, Ketter R, Weiler M, et al. Prognostic or predictive value of MGMT promoter methylation in gliomas depends on IDH1 mutation. *Neurology.* 2013;81:1515–22.
9. Wu T, Dai Y. Tumor microenvironment and therapeutic response. *Cancer Lett.* 2017;387:61–8.
10. Ni J, Liu S, Qi F, Li X, Yu S, Feng J, Zheng Y. Screening TCGA database for prognostic genes in lower grade glioma microenvironment. *Ann Transl Med.* 2020;8:209.
11. Yoshihara K, Shahmoradgoli M, Martinez E, Vegesna R, Kim H, Torres-Garcia W, Trevino V, Shen H, Laird PW, Levine DA, et al. Inferring tumour purity and stromal and immune cell admixture from expression data. *Nat Commun.* 2013;4:2612.
12. Shah N, Wang P, Wongvipat J, Karthaus WR, Abida W, Armenia J, Rockowitz S, Drier Y, Bernstein BE, Long HW, et al: Regulation of the glucocorticoid receptor via a BET-dependent enhancer drives antiandrogen resistance in prostate cancer. *Elife* 2017, 6.
13. Alonso MH, Ausso S, Lopez-Doriga A, Cordero D, Guino E, Sole X, Barenys M, de Oca J, Capella G, Salazar R, et al. Comprehensive analysis of copy number aberrations in microsatellite stable colon cancer in view of stromal component. *Br J Cancer.* 2017;117:421–31.
14. Gieryng A, Pszczolkowska D, Walentynowicz KA, Rajan WD, Kaminska B. Immune microenvironment of gliomas. *Lab Invest.* 2017;97:498–518.
15. Vismara MFM, Donato A, Malara N, Presta I, Donato G. Immunotherapy in gliomas: Are we reckoning without the innate immunity? *Int J Immunopathol Pharmacol.* 2019;33:2058738419843378.
16. Simonelli M, Persico P, Perrino M, Zucali PA, Navarria P, Pessina F, Scorsetti M, Bello L, Santoro A. Checkpoint inhibitors as treatment for malignant gliomas: "A long way to the top". *Cancer Treat Rev.* 2018;69:121–31.
17. Ascierto ML, Kmiecik M, Idowu MO, Manjili R, Zhao Y, Grimes M, Dumur C, Wang E, Ramakrishnan V, Wang XY, et al. A signature of immune function genes associated with recurrence-free survival in breast cancer patients. *Breast Cancer Res Treat.* 2012;131:871–80.
18. Kim K, Jeon S, Kim TM, Jung CK. Immune Gene Signature Delineates a Subclass of Papillary Thyroid Cancer with Unfavorable Clinical Outcomes. *Cancers (Basel)* 2018, 10.
19. Shen S, Wang G, Zhang R, Zhao Y, Yu H, Wei Y, Chen F. Development and validation of an immune gene-set based Prognostic signature in ovarian cancer. *EBioMedicine.* 2019;40:318–26.

20. Yang W, Lai Z, Li Y, Mu J, Yang M, Xie J, Xu J. Immune signature profiling identified prognostic factors for gastric cancer. *Chin J Cancer Res.* 2019;31:463–70.
21. Zhang M, Wang X, Chen X, Zhang Q, Hong J. Novel Immune-Related Gene Signature for Risk Stratification and Prognosis of Survival in Lower-Grade Glioma. *Front Genet.* 2020;11:363.
22. Cheng W, Ren X, Zhang C, Cai J, Liu Y, Han S, Wu A. Bioinformatic profiling identifies an immune-related risk signature for glioblastoma. *Neurology.* 2016;86:2226–34.
23. Leek JT, Scharpf RB, Bravo HC, Simcha D, Langmead B, Johnson WE, Geman D, Baggerly KA, Irizarry RA. Tackling the widespread and critical impact of batch effects in high-throughput data. *Nat Rev Genet.* 2010;11:733–9.
24. Xiong Y, Liu L, Bai Q, Xia Y, Qu Y, Wang J, Guo J: Individualized immune-related gene signature predicts immune status and oncologic outcomes in clear cell renal cell carcinoma patients. *Urologic Oncology: Seminars and Original Investigations* 2020, 38:7.e1-7.e8.
25. Sun XY, Yu SZ, Zhang HP, Li J, Guo WZ, Zhang SJ. A signature of 33 immune-related gene pairs predicts clinical outcome in hepatocellular carcinoma. *Cancer Med.* 2020;9:2868–78.
26. Chen W, Ou M, Tang D, Dai Y, Du W: Identification and Validation of Immune-Related Gene Prognostic Signature for Hepatocellular Carcinoma. *J Immunol Res* 2020, 2020:5494858.
27. Wu J, Zhao Y, Zhang J, Wu Q, Wang W. Development and validation of an immune-related gene pairs signature in colorectal cancer. *Oncoimmunology.* 2019;8:1596715.
28. Zhang L, Zhu P, Tong Y, Wang Y, Ma H, Xia X, Zhou Y, Zhang X, Gao F, Shu P. An immune-related gene pairs signature predicts overall survival in serous ovarian carcinoma. *OncoTargets Therapy.* 2019;12:7005–14.
29. Li B, Cui Y, Diehn M, Li R. Development and Validation of an Individualized Immune Prognostic Signature in Early-Stage Nonsquamous Non-Small Cell Lung Cancer. *JAMA Oncol.* 2017;3:1529–37.
30. Ritchie ME, Phipson B, Wu D, Hu Y, Law CW, Shi W, Smyth GK: limma powers differential expression analyses for RNA-sequencing and microarray studies. *Nucleic Acids Res.* 2015;43:e47.
31. Newman AM, Liu CL, Green MR, Gentles AJ, Feng W, Xu Y, Hoang CD, Diehn M, Alizadeh AA. Robust enumeration of cell subsets from tissue expression profiles. *Nat Methods.* 2015;12:453–7.
32. Chen H, Boutros PC. VennDiagram: a package for the generation of highly-customizable Venn and Euler diagrams in R. *BMC Bioinformatics.* 2011;12:35.
33. Kiran M, Chatrath A, Tang X, Keenan DM, Dutta A. A Prognostic Signature for Lower Grade Gliomas Based on Expression of Long Non-Coding RNAs. *Mol Neurobiol.* 2019;56:4786–98.
34. Deng X, Lin D, Zhang X, Shen X, Yang Z, Yang L, Lu X, Yu L, Zhang N, Lin J. Profiles of immune-related genes and immune cell infiltration in the tumor microenvironment of diffuse lower-grade gliomas. *J Cell Physiol* 2020.
35. Persano L, Pistollato F, Rampazzo E, Della Puppa A, Abbadi S, Frasson C, Volpin F, Indraccolo S, Scienza R, Basso G. BMP2 sensitizes glioblastoma stem-like cells to Temozolomide by affecting HIF-1 α stability and MGMT expression. *Cell Death Dis.* 2012;3:e412.

36. Ishihara E, Takahashi S, Fukaya R, Ohta S, Yoshida K, Toda M. Identification of KLRC2 as a candidate marker for brain tumor-initiating cells. *Neurol Res.* 2019;41:1043–9.
37. Uemae Y, Ishikawa E, Osuka S, Matsuda M, Sakamoto N, Takano S, Nakai K, Yamamoto T, Matsumura A. CXCL12 secreted from glioma stem cells regulates their proliferation. *J Neurooncol.* 2014;117:43–51.
38. Fecci PE, Mitchell DA, Whitesides JF, Xie W, Friedman AH, Archer GE, Herndon JE 2nd, Bigner DD, Dranoff G, Sampson JH. Increased regulatory T-cell fraction amidst a diminished CD4 compartment explains cellular immune defects in patients with malignant glioma. *Cancer Res.* 2006;66:3294–302.
39. Alexiou GA, Vartholomatos G, Karamoutsios A, Batistatou A, Kyritsis AP, Voulgaris S. Circulating progenitor cells: a comparison of patients with glioblastoma or meningioma. *Acta Neurol Belg.* 2013;113:7–11.
40. Wainwright DA, Dey M, Chang A, Lesniak MS. Targeting Tregs in Malignant Brain Cancer: Overcoming IDO. *Front Immunol.* 2013;4:116.

Figures

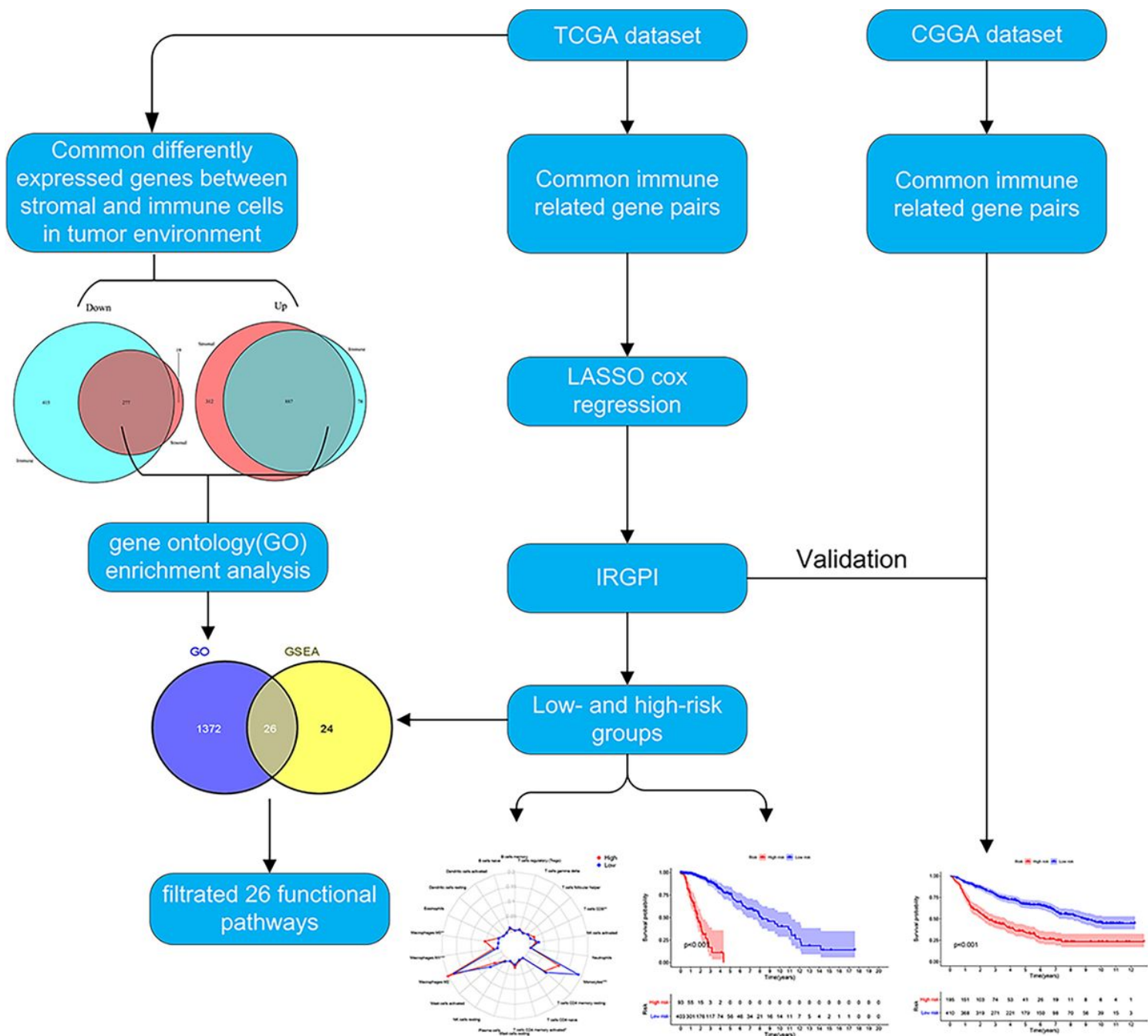


Figure 1

The workflow describes the construction of our investigation process. The TCGA data were assigned to a training dataset, and the training dataset was used to construct immune-related gene pair signatures. The CGGA datasets were used to validate the IRGPI. The 26 functional pathways were filtrated by the intersection of GO and GSEA in TCGA dataset.

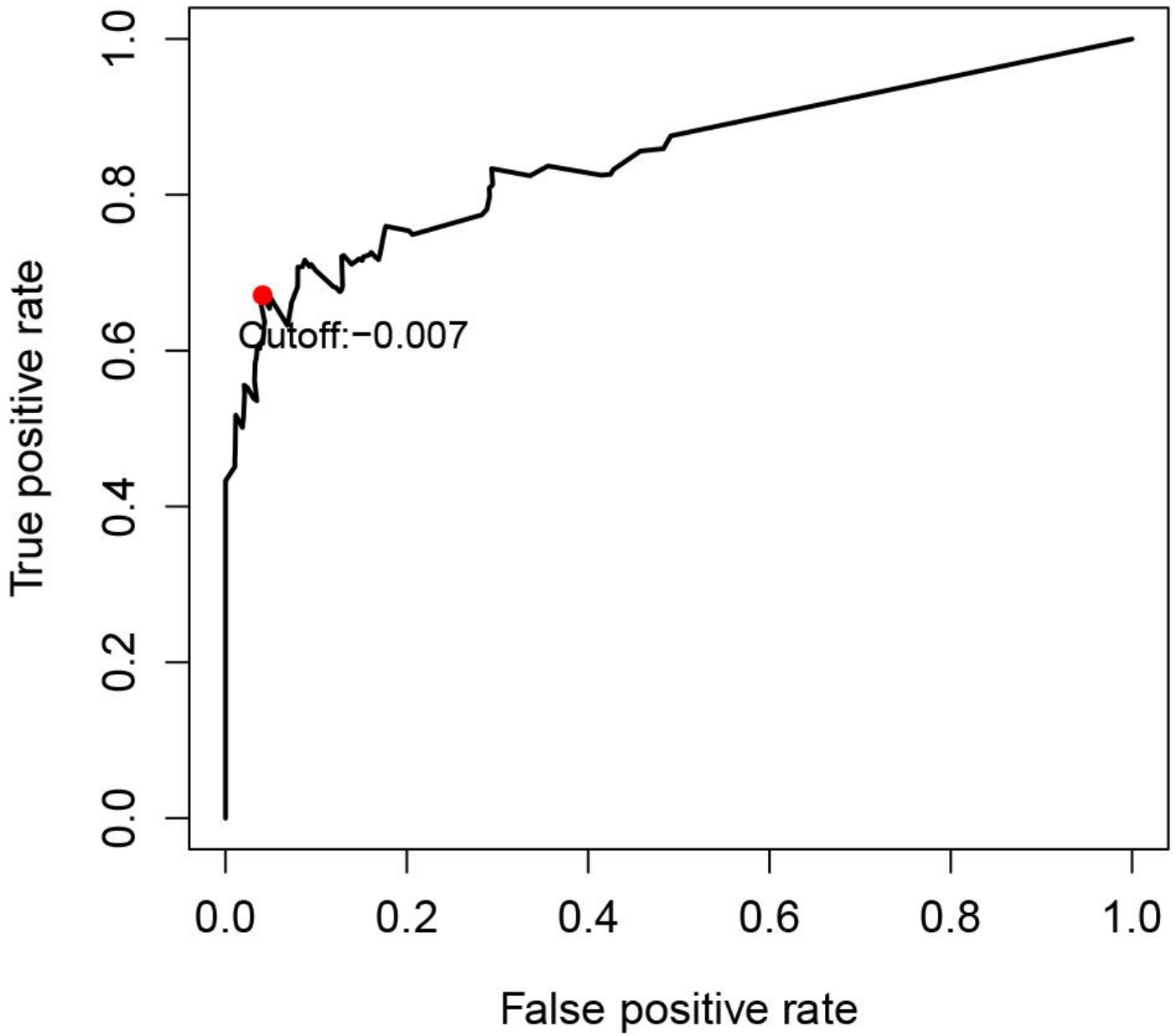


Figure 2

Time-dependent ROC curve for IRGPI in the TCGA dataset. IRGPI score of -0.007 was used as the optimal cut-off for IRGPI to stratify patients into low- or high-risk groups.

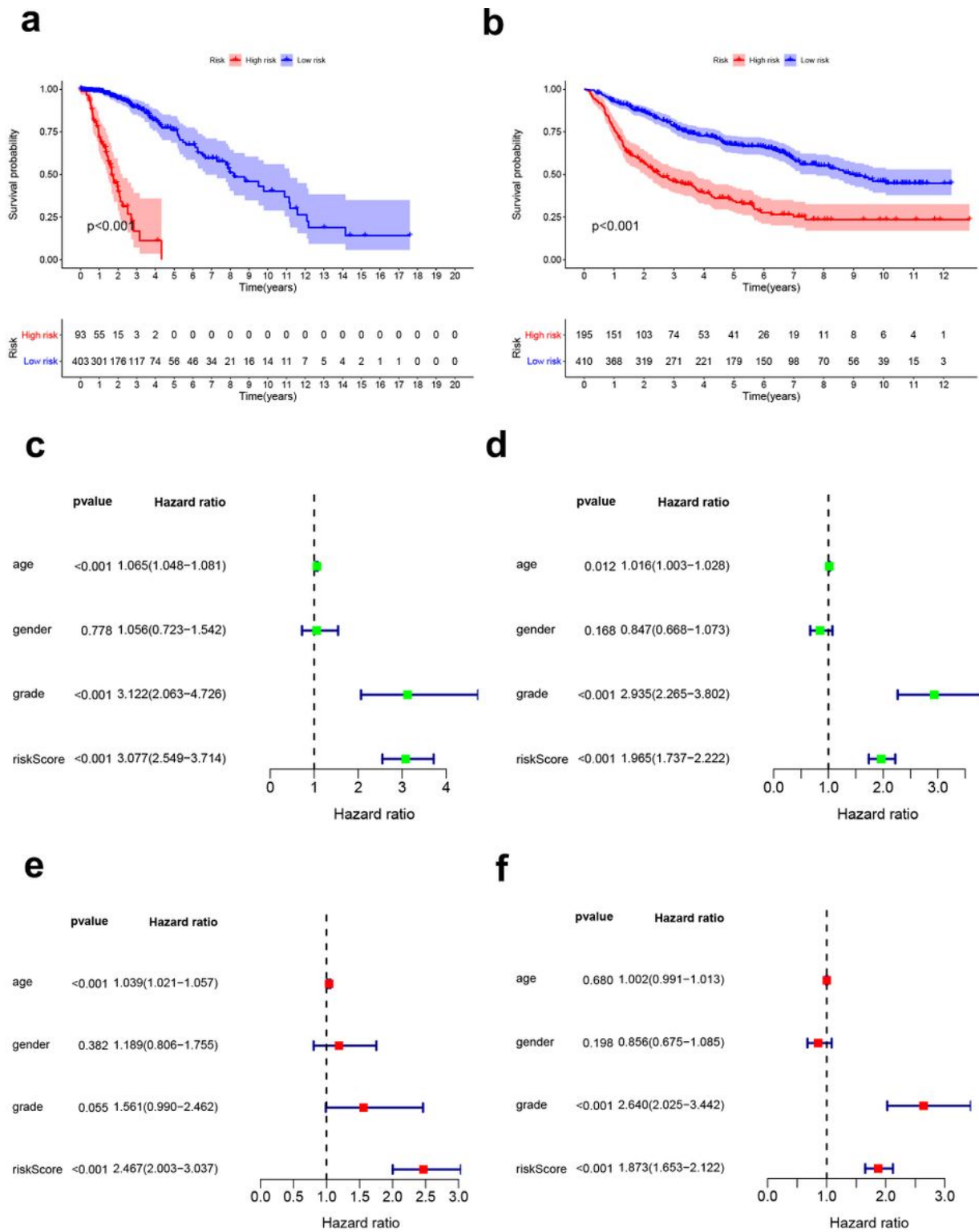


Figure 3

Analysis of survival and independent prognostic factors. Kaplan-Meier curves of overall survival (OS) among different IRGPI risk groups (low vs high risk). OS among patients in the training (a) and validation cohorts (b). The risk score of IRGPI was an independent prognostic factor among univariate (c) and multivariate(e) analyses in the TCGA database. The risk score of IRGPI was also an independent prognostic factor among univariate (d) and multivariate(f) analyses in CGGA dataset.

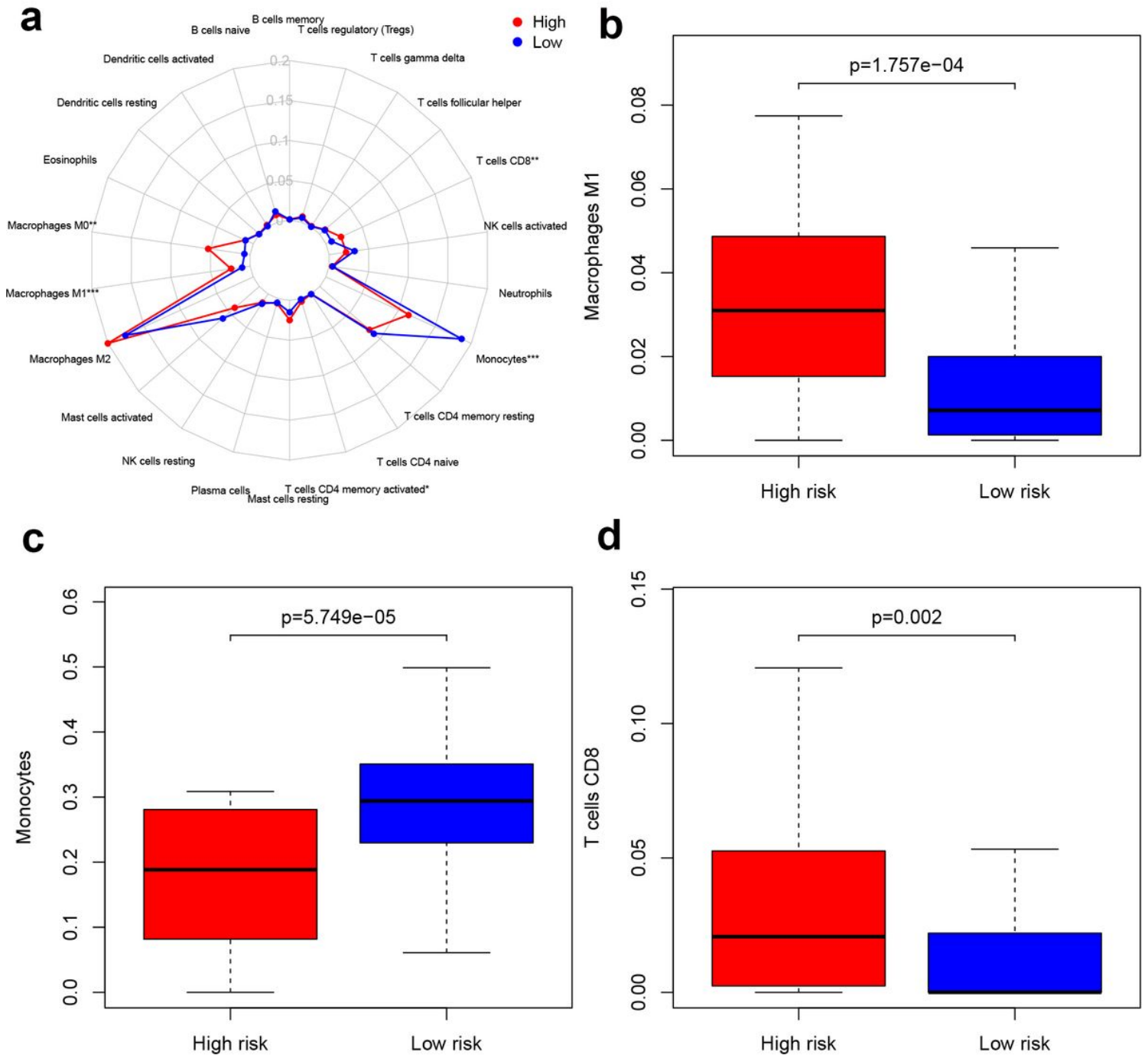


Figure 4

Immune infiltration situation between IRGPI risk groups. (a) Summary of the outcome estimated by CIBERSORT in different risk groups. (b) Macrophages M1 was significantly highly expressed in the high-risk group ($P=1.757e-04$). (c) Monocytes were significantly highly expressed in the low-risk group ($P=5.749e-05$). (d) T cells CD8 was significantly highly expressed in the high-risk group ($P=0.002$). P-values are based on t-test (* $P<0.05$, ** $P<0.01$, *** $P<0.001$).

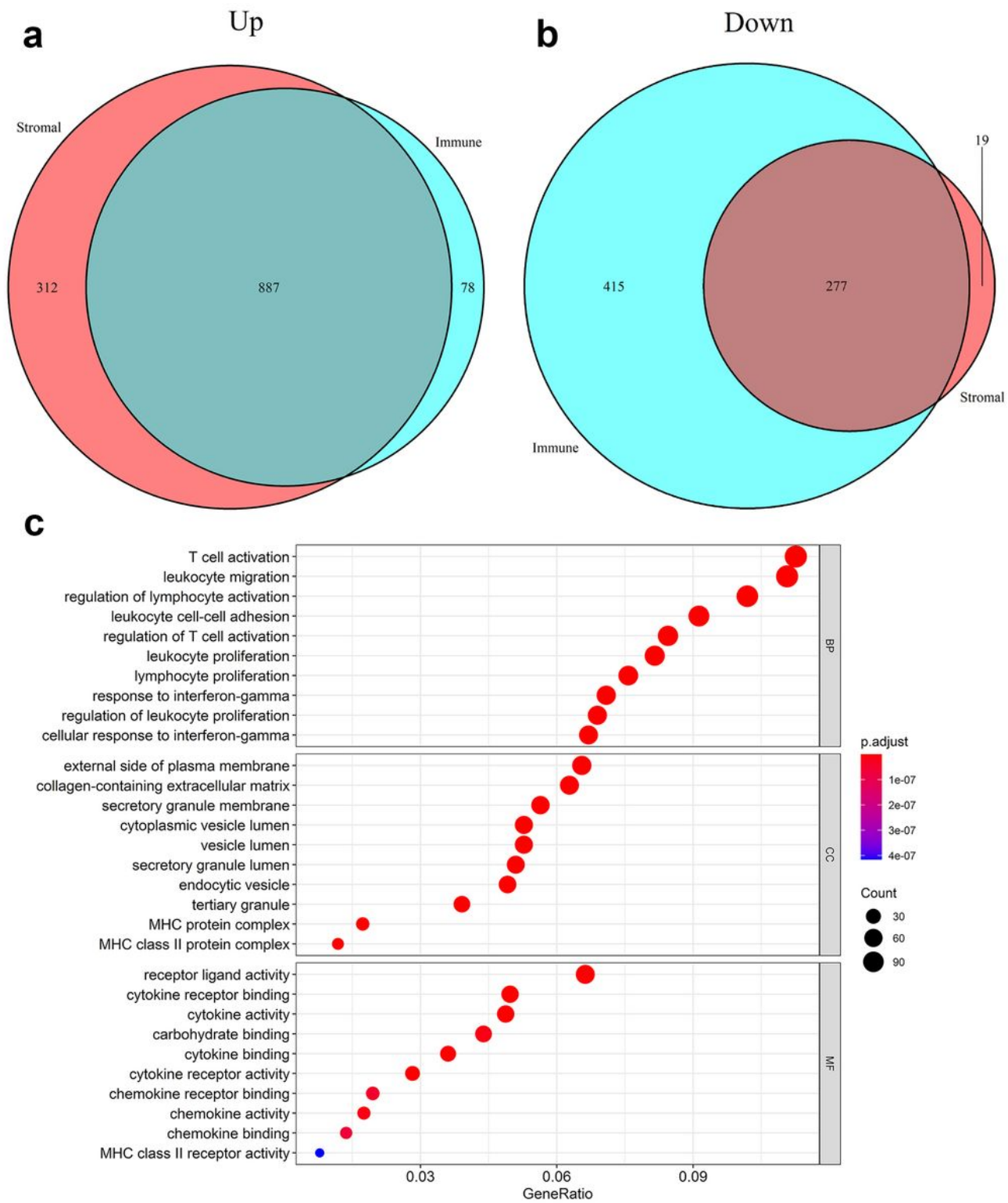


Figure 5

Differentially expressed genes analyses in TCGA dataset. (a) 887 up-regulated intersected genes and (b) 277 down-regulated intersected genes were revealed in venn plots.

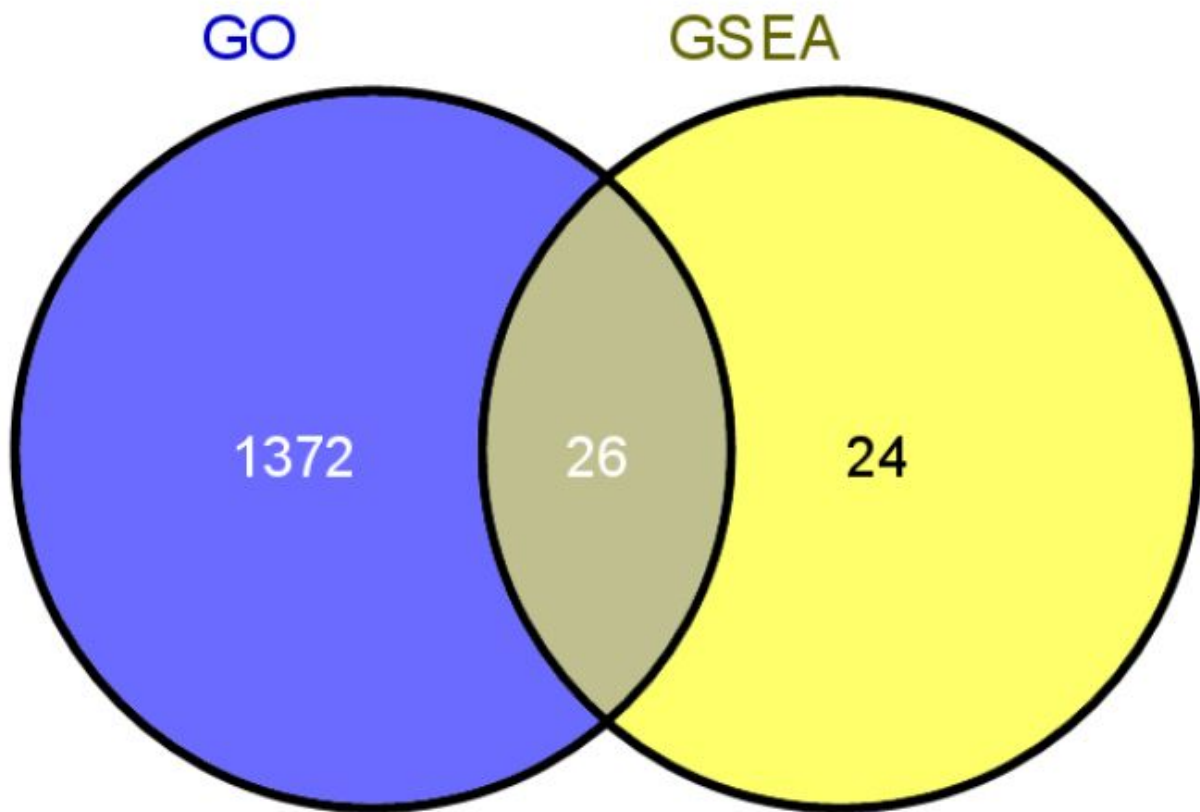


Figure 6

The intersection between GO and GSEA, 26 functional pathways were filtrated.

Supplementary Files

This is a list of supplementary files associated with this preprint. Click to download.

- [Additionalfile3FigS1.jpg](#)
- [Additionalfile2TableS2.docx](#)
- [Additionalfile1TableS1.docx](#)